Aeroelastic Analyses with Uncertainty in Structural Properties

Marc P. Mignolet[1] and Ping Chih Chen[2]

[1]Department of Mechanical and Aerospace Engineering
Arizona State University, Tempe, AZ 85287, USA

[2]ZONA Technology, Inc., 9489 E. Ironwood Square Drive
Scottsdale, AZ 85258, USA

marc.mignolet@asu.edu and pc@zonatech.com

ABSTRACT

This paper focuses on the introduction in aeroelastic analyses of uncertainties in the structural model arising from the modeling of the real structure (model uncertainty) and/or from variability in the structural properties from one aircraft to another (data uncertainty). This effort relies on a recently introduced methodology, referred to as the nonparametric stochastic modeling method, which is first briefly reviewed. Next, its applicability to various aeroelastic analyses of uncertain wings and panels is described. Considered first is the flutter analysis of the Goland wing with uncertainty in either the structural properties or its boundary conditions. A second set of aeroelastic analyses is carried out for uncertain panels in a supersonic flow. Specifically, the variability of the corresponding panel flutter boundary and of its forced response to an acoustic excitation is first obtained using a linear nonparametric stochastic structural dynamic model of the panel. Adopting finally a geometrically nonlinear uncertain structural dynamic model permits the assessment of the variability of the limit cycle oscillation amplitude and forced response of the panel in post-flutter conditions. These various applications demonstrate the broad applicability of the nonparametric stochastic modeling method for the aeroelastic analysis of uncertain aircraft and aircraft components.

1 INTRODUCTION

The accurate prediction of the aeroelastic behavior of aircraft and aircraft components (i.e. wings, panels, etc.), e.g. flutter boundary, amplitude of limit cycle oscillations, forced response to acoustic/gust excitation, necessitates several key elements. Certainly, it is necessary to dispose of reliable algorithms/methods for the solution of the governing equations of the fluid and structure and many efforts has been devoted to this issue in the last decades. While improvements in these algorithms and methods are still on-going, it now appears that small differences between the actual structure considered and its computational structural model may represent the next limiting factor in the matching between computed and actual aeroelastic responses. This finding seems surprising at first given the flexibility and power of the finite element methodology. Note however that a finite element model of a structure always remains a *model* and thus neglects or approximates certain structural features. For example, rivets are typically not considered in the discretization and the computational boundary conditions typically only approximate their true counterparts. Additional sources of unknown discrepancies are the detailed geometry, the likely lack of a perfect isotropy, etc. There is thus an innate uncertainty associated with the modeling effort, usually referred to as modeling uncertainty. Model updating will generally minimize this uncertainty but cannot completely eliminate it since, for example, the

Mignolet, M.P.; Chen, P.C. (2007) Aeroelastic Analyses with Uncertainty in Structural Properties. In *Computational Uncertainty in Military Vehicle Design* (pp. 2-1 – 2-18). Meeting Proceedings RTO-MP-AVT-147, Paper 2. Neuilly-sur-Seine, France: RTO. Available from: http://www.rto.nato.int.

response of an orthotropic structure cannot be exactly matched by that of an isotropic structure. A second source of uncertainty is the manufacturing process, i.e. no two parts can be produced which are perfectly identical. Thus, parts will differ from each other by their mechanical properties (Young's modulus, Poisson's ratio) and/or geometry (including panel thickness) which are collectively referred to as data uncertainty as these quantities represent the data of the computational structural model.

Having clarified the existence of model and data uncertainties and suggested that it limits the accuracy of the matching between predicted and actual aeroelastic response, it remains to devise a strategy for the incorporation of uncertainty in aeroelastic analyses. In this regard, its unpredictability and variability from part to part suggest its modeling in terms of random (or stochastic) variables and processes. The next question to address concerns the level of analysis at which this modeling must take place. Specifically, should uncertainty be introduced at the finite element level or, since aeroelastic analyses are often conducted by expanding the structural response in terms of modes, directly at the modal model level? Certainly, both options are possible. The introduction of the uncertainty at the finite element level is preferable when it is known which model data, e.g. geometrical and/or material properties, are uncertain and when an accurate statistical description of these random variables, processes, and fields is available or can be assumed. Also fall in this category analyses that seek to relate the uncertainty on the response to variations in specific model data. Since the uncertainty affects specific parameters of the physical/finite element model, this approach is referred to as parametric. When little is known about the exact sources of uncertainty (e.g. which parameters, what statistical distribution to adopt, etc.), it is more convenient to proceed directly at the modal model level relying on the nonparametric method initially developed by Soize, see [1-4] and review below. This approach is termed nonparametric as it does not focus the uncertainty on specific parameters of the finite element model and, as such, it can also address the consideration of *model* uncertainty, as described above, at the contrary of the finite element level implementation which is achieved on a fixed model.

Two key points which must be addressed in a modal level implementation are (i) which set of "modes" to use, and (ii) which statistical distributions to adopt for the random modal model properties. This latter question will be discussed in detail in the next section and a summary of the approach devised in references [1,2] will be presented. The former question however, i.e. the choice of modes, is more straightforward. A first notable choice is to use the random modes associated with an underlying random finite element model. While this choice leads to diagonal mass and stiffness matrices, it is however quite challenging to simulate these random modes directly without having to extract them from a full finite element model (which would be the strategy followed in a parametric approach). The main difficulty in such a direct simulation is the need to satisfy explicitly the orthogonality conditions with respect to the unspecified random mass and stiffness matrices of the underlying full model. A better alternative is to use a fixed set of modes, e.g. those corresponding to the design computational model (see [5] for the consideration of uncertainty on boundary conditions). Not only does this choice of modes eliminates the difficult simulation step discussed above but it also fits naturally in aeroelastic analyses with linear aerodynamics since the generalized aerodynamic forces need then to be computed only once. Since the modes used are not those of the underlying random structure, the modal equations will not be uncoupled and one needs to generate random full mass and stiffness matrices. The approach developed in references [1-4] for this simulation is summarized below.

2 SIMULATION OF RANDOM MATRICES BY ENTROPY MAXIMIZATION

Following the discussion of the previous section, the fundamental problem of the nonparametric approach is the simulation of random symmetric positive definite real matrices. In uncertain linear structural models, they are the mass, damping, and/or stiffness matrices of the modal model but such a problem is also central to the

introduction of uncertainty in nonlinear geometric structural models. Specifically, it has been shown, see for example reference [3], that the generic form of a reduced order model for a linearly elastic (in the sense of the second Piola-Kirchhoff stress and Green strain tensors) is

$$M_{ij}\,\ddot{q}_j + C_{ij}\,\dot{q}_j + K^{(1)}_{ij}\,q_j + K^{(2)}_{ijl}\,q_j\,q_l + K^{(3)}_{ijlp}\,q_j\,q_l\,q_p = F_i \tag{1}$$

where summation is implied over repeated indices. In the above equation, q_i denote the generalized coordinates, M_{ij} and C_{ij} are mass and damping coefficients, and F_i denotes the external modal forces transported to the reference configuration. Finally, $K^{(1)}_{ij}$, $K^{(2)}_{ijl}$, $K^{(3)}_{ijlp}$ denote the linear, quadratic, and cubic stiffness coefficients. Under very broad conditions (see [3]), it is found that the matrix

$$\underline{\underline{K}}_B = \begin{bmatrix} \underline{\underline{K}}^{(1)} & \underline{\underline{\widetilde{K}}}^{(2)} \\ \underline{\underline{\widetilde{K}}}^{(2)T} & 2\underline{\underline{\widetilde{K}}}^{(3)} \end{bmatrix} \tag{2}$$

is, besides symmetric, also positive definite. In this definition, $\underline{\underline{K}}^{(1)}$ is the linear stiffness matrix of elements $K^{(1)}_{ij}$ while $\underline{\underline{\widetilde{K}}}^{(2)}$ and $\underline{\underline{\widetilde{K}}}^{(3)}$ are matrices obtained by "reshaping" (see [3]) the third and fourth order tensors of components $K^{(2)}_{ijl}$ and $K^{(3)}_{ijlp}$, respectively. Thus, the consideration of uncertainty in the "stiffness" properties of a geometrically nonlinear system will be achieved by first simulating symmetric positive definite random matrices $\underline{\underline{K}}_B$, then extracting the corresponding $\underline{\underline{K}}^{(1)}$, $\underline{\underline{\widetilde{K}}}^{(2)}$, and $\underline{\underline{\widetilde{K}}}^{(3)}$, and finally reshaping the latter two matrices to obtain the elements $K^{(2)}_{ijl}$ and $K^{(3)}_{ijlp}$.

Having established the importance of simulating random symmetric positive definite matrices $\underline{\underline{A}}$, it remains to specify which (joint) statistical distribution of their elements A_{ij} should be adopted. In this regard, it will first be assumed that the mean of the random matrix $\underline{\underline{A}}$ is known as $\overline{\underline{\underline{A}}}$, i.e. $E\left[\underline{\underline{A}}\right] = \overline{\underline{\underline{A}}}$ where $E[.]$ denotes the operation of mathematical expectation. If, as discussed above, the fixed modes used to represent the motion of the uncertain structures are those associated with the mean structural model (also referred to as the design conditions model) and are mass normalized, then the mean of the random mass and stiffness matrices are the identity matrix and the diagonal matrix of the squared natural frequencies, respectively. Further, if the mean model does not exhibit any rigid body mode (i.e. $\overline{\underline{\underline{A}}}$ is strictly positive definite), then it is also expected that the random matrices $\underline{\underline{A}}$ will share the same property (note that the extension of the methodology to mean models exhibiting rigid body modes has been accomplished in [5]). This condition is equivalent to the existence of a flat zero at zero of the probability density function of the eigenvalues of $\underline{\underline{A}}$. Finally, it will be assumed that only a single measure of the variability of the matrices $\underline{\underline{A}}$ is available, e.g. the standard deviation of the lowest eigenvalue of $\underline{\underline{A}}$ (the extension of the methodology to account for multiple known measures of variability has been accomplished in [4]).

Even with the above assumptions (known mean model, nonsingularity of $\underline{\underline{A}}$, and known measure of variability), there is a broad set of statistical distributions of the elements A_{ij} that could be selected. Among those, it would be particularly desirable to select the one that places particular emphasis on "larger" deviations

from the mean value, a desirable feature to assess, in a limited Monte Carlo study, the aeroelastic robustness of a design to uncertainty. As discussed in references [1-4], this property is achieved by the distribution of the elements A_{ij} that achieves the *maximum of the statistical entropy* under the stated constraints of symmetry, positive definiteness, known mean model, nonsingularity of $\underline{\underline{A}}$, and known measure of variability. This maximum is satisfied (see [1-4]) when the matrices $\underline{\underline{A}}$ are generated as

$$\underline{\underline{A}} = \overline{\underline{\underline{L}}}\ \underline{\underline{H}}\ \underline{\underline{H}}^T\ \overline{\underline{\underline{L}}}^T \tag{3}$$

where $\overline{\underline{\underline{L}}}$ is any decomposition, e.g. Cholesky, of $\overline{\underline{\underline{A}}}$, i.e. satisfying $\overline{\underline{\underline{A}}} = \overline{\underline{\underline{L}}}\ \overline{\underline{\underline{L}}}^T$. Further, $\underline{\underline{H}}$ denotes a lower triangular random matrix the elements of which are all statistically independent of each other. Moreover, the probability density functions of the diagonal (H_{ii}) and off-diagonal elements (H_{il}) are

$$p_{H_{ii}}(h) = C_{ii}\, h^{p(i)} \exp\left[-\mu h^2\right] \ , \ h \geq 0 \tag{4}$$

and

$$p_{H_{il}}(h) = C_{il}\ \exp\left[-\mu h^2\right] \ , \ h \geq 0 \ , \ i \neq l \tag{5}$$

where

$$p(i) = n - i + 2\lambda - 1 \qquad \mu = \frac{n + 2\lambda - 1}{2} \tag{6}$$

$$C_{ii} = \frac{2\mu^{[p(i)+1]/2}}{\Gamma\left(\left(p(i)+1\right)/2\right)} \qquad C_{il} = \sqrt{\frac{\mu}{\pi}} \tag{7}$$

In these equations, n denotes the size of the matrices $\underline{\underline{A}}$, i.e. the number of modes retained, and $\Gamma(.)$ denotes the Gamma function. In fact, it is readily seen that (see also Fig. 1):

(1) the off-diagonal elements H_{il}, $i \neq l$, are normally distributed (Gaussian) random variables with standard deviation $\sigma = 1/\sqrt{2\mu}$,

and

(2) the diagonal elements H_{ii} are obtained as $H_{ii} = \sqrt{\frac{Y_{ii}}{\mu}}$ where Y_{ii} is Gamma distributed with parameter $\left(p(i)-1\right)/2$.

In the above equations, the parameter $\lambda > 0$ is the free parameter of the statistical distribution of the random matrices $\underline{\underline{H}}$ and $\underline{\underline{A}}$ and can be evaluated to meet any given information about their variability. In the ensuing examples, the standard deviation of the lowest natural frequency of the random linear system will be specified and used to obtain λ. This condition, coupled with Eqs (3)-(7), provides a complete scheme for the generation of random symmetric positive definite matrices $\underline{\underline{A}}$.

3 AEROELASTIC APPLICATION 1: GOLAND WING FLUTTER

The above concepts were first validated on the Goland wing [6,7] of Fig. 2 and Table 1 to assess the effects of structural uncertainty on its flutter boundary. All aeroelastic analyses were conducted with ZAERO with a modal model including the first 20 modes of the mean Goland wing and neglecting structural damping. The

mean Goland wing was first analyzed and was found to exhibit two flutter points at speeds of 752.87 ft/s (frequency of 1.966Hz) and 839.87 ft/s (frequency of 9.501Hz) and divergence at 781.49ft/s. Both first flutter and divergence modes are mostly combinations of the first two structural modes (with the first one dominant) while the higher speed flutter mode is dominated by the third and fourth (dominant) structural modes. The effects of structural uncertainty were analyzed next. A first set of random aeroelastic analyses were carried out assuming that the uncertainty affects solely the "stiffness properties" of the wing, not its clamped boundary condition. Further, the formulation of Eqs (3)-(7) was adopted to simulate the random stiffness matrices and the parameter λ was selected so that the random Goland wings would exhibit a standard deviation of the first natural frequency equal to 1% of its value for the mean model (i.e. 1.690Hz). An ensemble of 300 such stiffness matrices were generated and for each matrix/wing, a matched point flutter analysis was conducted with ZAERO for M_∞=0.7. Of the 300 uncertain Goland wings thus simulated, 13 were found to exhibit first divergence while the remaining 287 fluttered first. Shotgun plots of the results are presented in Fig. 3 together with the results of the design conditions (or mean) wing (lower flutter and divergence speeds). Note on Fig. 3(b) that the divergence cases form two distinct groups exhibiting very similar mode shapes but separated speed ranges. In regards to the mode shapes, note that their component with respect to the 2nd mean structural mode (with the component of the first mean structural mode normalized to 1) is well correlated to the flutter frequency (see Fig. 3(c)), as can be expected from an eigenvalue problem. Accordingly, the speed and frequency represent the two fundamental variables which will be investigated in the sequel.

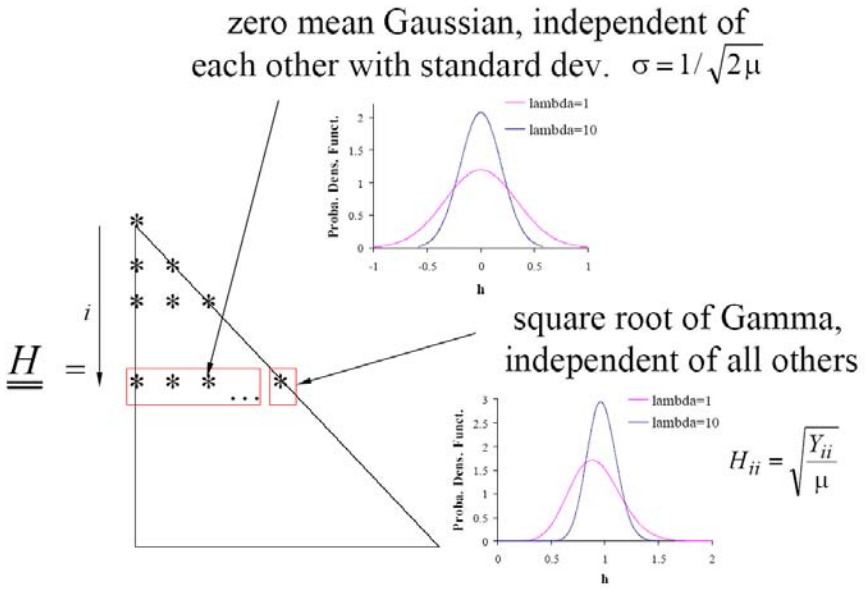

Figure 1: Structure of the random $\underline{\underline{H}}$ matrices (figures for *n*=8, *i*=2, and λ=1 and 10)

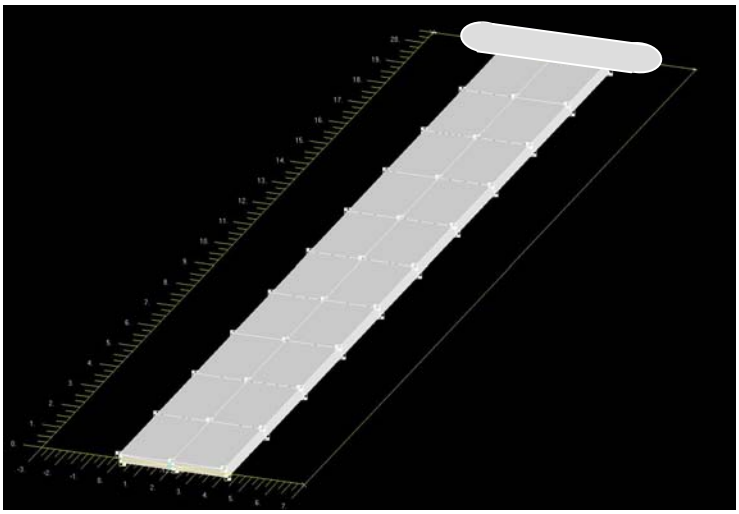

Figure 2: Goland wing structural model

Table 1. Natural frequencies of the mean (design conditions) Goland wing

Mode #	Nat. Freq. (Hz)	Mode #	Nat. Freq. (Hz)
1	1.690	6	16.260
2	3.051	7	22.845
3	9.172	8	26.318
4	10.834	9	29.183
5	11.258		

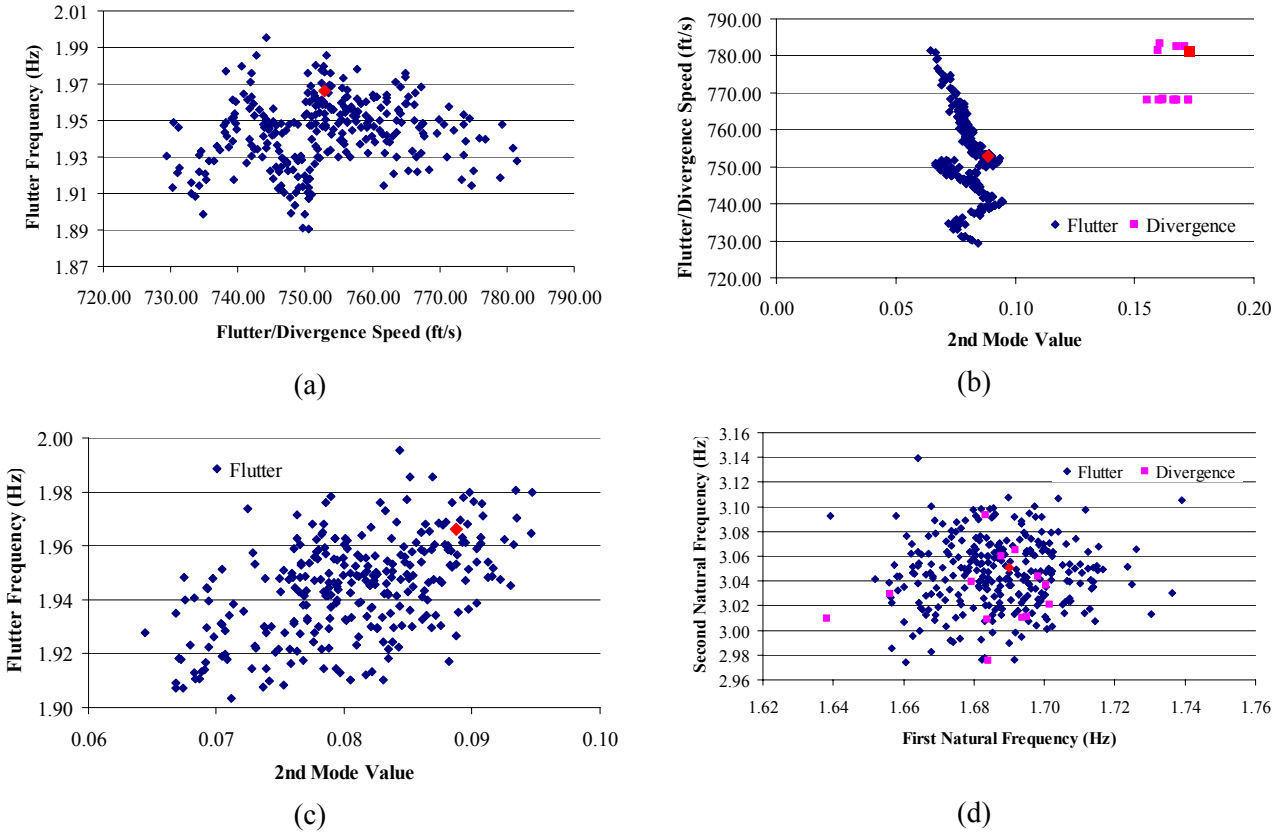

Figure 3. Shotgun plots of (a) flutter frequency vs. flutter speed (flutter results only), (b) component of the 2nd mean structural mode in the flutter and divergence modes, (c) flutter frequency vs. component of the 2nd mean structural mode in the flutter mode (flutter results only), (d) first two natural frequencies of the random wings. The red triangle/square denote the design conditions (flutter/divergence)

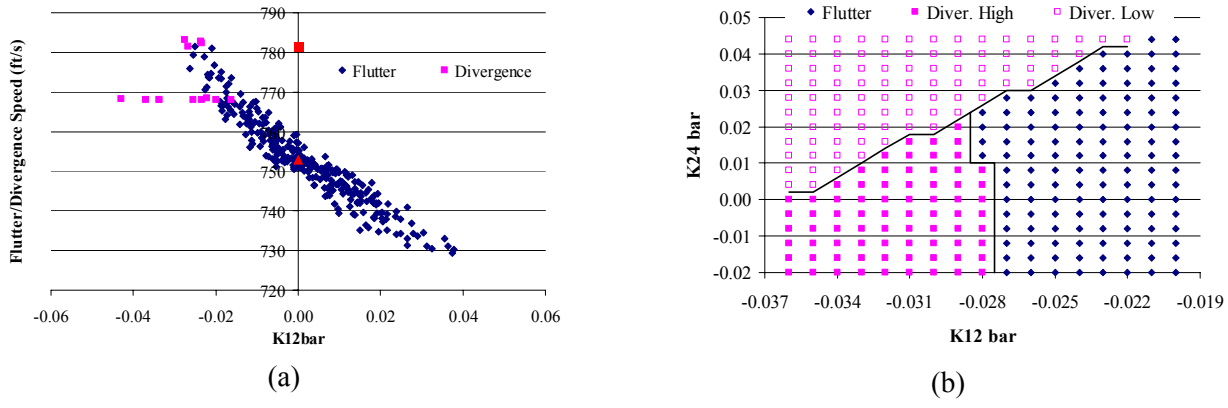

Figure 4. (a) Shotgun plot of the flutter speed vs. normalized stiffness coefficient $\overline{K}_{12}$. (b) Nature of aeroelastic instability as function of the dimensionless stiffnesses $\overline{K}_{12}$ and $\overline{K}_{24}$. The red triangle/square denote the design conditions (flutter/divergence).

In search for a clarification of these observations, the first two natural frequencies of the random Goland wings were first analyzed, see Fig. 3(d), but these variables do not appear to justify why certain cases led to divergence and others to flutter. In fact, this finding is expected: since the flutter mechanism of the mean Goland wing is based on the *aerodynamic coupling* of the first bending and torsion modes, it is the structural coupling of these modes induced by uncertainty which should be suspected to be the most significant parameter. This expectation is confirmed in Fig. 4(a) which demonstrates that the flutter speed correlates very well indeed with the stiffness K_{12} or its dimensionless counterpart

$$\overline{K}_{12} = \frac{K_{12}}{\sqrt{K_{11}\, K_{22}}}. \tag{8}$$

Note in particular that the divergence cases correspond to "large" negative values of K_{12}, i.e. the flutter is impeded by this coupling between the 2 modes (thus justifying the increase in flutter speed with decreasing K_{12} value) but divergence is promoted by such values. This difference in behavior originates from the opposite signs of the components of the second mean structural mode in the flutter and divergence modes.

While the aeroelastic behavior of the 300 uncertain wings can be globally explained by $\overline{K}_{12}$, not all issues can be clarified through this parameter. For example, for values of $\overline{K}_{12}$ in the range [-0.026,-0.016], both flutter and divergence may occur. Further divergence may occur either upward of 780 ft/s or at approximately 769 ft/s. These findings suggest that one or several other stiffness parameters have a noticeable, albeit less significant, role. Since the 4th structural mode (the second torsion mode) is, after the first two, the largest contributor to the flutter/divergence modes, the correlation of the above findings with K_{14} and K_{24} was next investigated. In fact, it was found that the combined knowledge of $\overline{K}_{12}$ and $\overline{K}_{24}$ (defined as in Eq. (8)) does allow the prediction of the nature of the aeroelastic instability: flutter, low speed divergence (i.e. at a speed approximately 769 ft/s), or high speed divergence (i.e. at a speed higher than 780 ft/s), as demonstrated in Fig. 4(b). Thus, the qualitative aspects of the aeroelastic response of uncertain Goland wings are dominated by the two stiffness coefficients K_{12} and K_{24}, with the first one playing the dominant role.

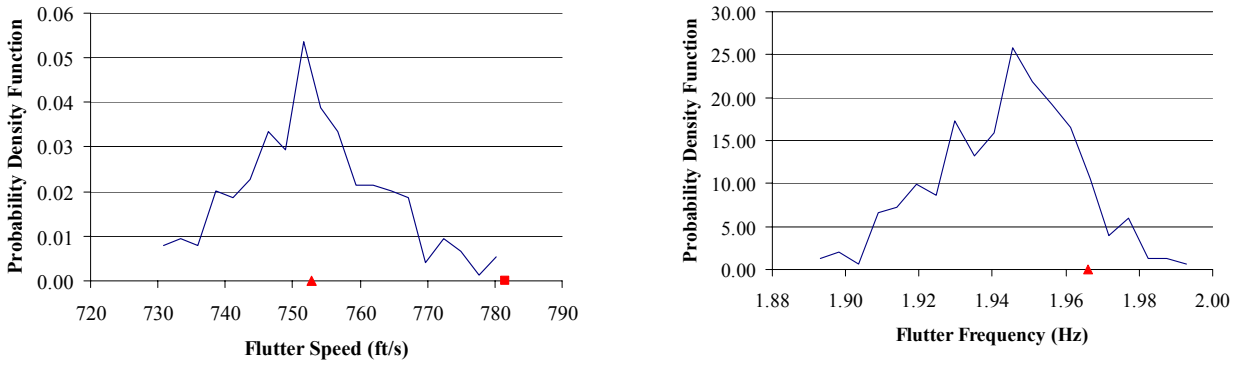

(a) (b)

Figure 5. Probability density functions of (a) the flutter speed and (b) the flutter frequency. The red triangle/square denote the design conditions (flutter/divergence).

Turning next to the quantitative analysis of the effects of structural uncertainty on the aeroelastic response of the Goland wing, shown in Fig. 5 are the probability density functions of the flutter speed and frequency estimated from the above 287 cases. It is seen from these figures that the distribution of the flutter speed is

approximately symmetric around the mean wing flutter speed (mean flutter speed = 752.78 ft/s vs. flutter speed of mean wing = 752.87 ft/s) and extend till the divergence speed, as also clear from Fig. 4(a). The distribution of the flutter frequency however appears skewed with a higher emphasis on the low tail leading to a mean frequency of 1.94Hz vs. the flutter frequency of the mean wing of 1.97Hz.

The "standard" nonparametric approach, i.e. as described in Eqs (4)-(7) and exemplified in Figs 3-5, relies on the specification of a single measure of variability (the standard deviation of the first natural frequency in the Goland wing application) which is particularly advantageous when very little information or none exists on the level of uncertainty. Then, the scant data known can be used to determine the coefficient λ or a parametric study can be conducted with respect to λ to assess the effects of uncertainty. In some cases however, a more detailed knowledge of the level of uncertainty is available (e.g. the standard deviation of the first three natural frequencies) and this information may not be compatible with Eqs (4)-(7) with a single value of λ. For example, it was observed in the above Goland wing application that the standard deviation of the second natural frequency is approximately also 1% of its value for the design wing (3.051Hz). Thus, the model of Eqs (4)-(7) cannot be used to produce random stiffness matrices that lead to standard deviations of the first two natural frequencies that are equal to 1.5% and 1% say of their design values, assuming that such an information is available. However, an extension of the nonparametric method has recently been carried out [4] that permits the imposition of $m \le n$ (n being the size of the random matrix) different measures of uncertainty, e.g. the standard deviations of m natural frequencies.

This extension of the nonparametric approach (see [4] for complete theoretical details) was applied to the Goland wing model of Fig. 2 and Table 1 with standard deviations of the first two natural frequencies being fixed at 1.5% and 1% (for case I) and 1% and 1.5% (for case II) of their values for the design wing (see Table 1). Two new ensembles of 300 stiffness matrices (no uncertainty on the mass matrix was considered) were generated according to the algorithm of reference [4] and the corresponding matched point flutter analyses were carried with ZAERO for all 600 random system for M_∞=0.7. Plotted in Fig. 6(a) is the ensemble of the first and second natural frequencies of the simulated wings which appropriately reflects a larger variability for the first frequency than for the second in case I and the reverse for case II. Although the variability of the first two natural frequencies has either remained the same (when 1%) or increased slightly (when 1.5%) as in the previous example, it was found that the number of cases in which divergence occurred increased significantly, from 13 in the previous set of computations to 34 for case I and 31 for case II, see Fig. 6(b) for case I (a completely similar picture was obtained for case II). Comparing Figs 4(a) and 6(b), it is seen that this increase in higher flutter frequency occurrence is identical in origin and can be traced to an sharp increase in the standard deviation of the normalized stiffness coefficient $\overline{K}_{12}$, from 0.015 in the first analysis (Figs 3 to 5) to 0.022 (for both cases I and II) as compared to 0.20 for the standard approach with a standard deviation of 1.5% of the first natural frequency and approximately the same value for the second frequency.

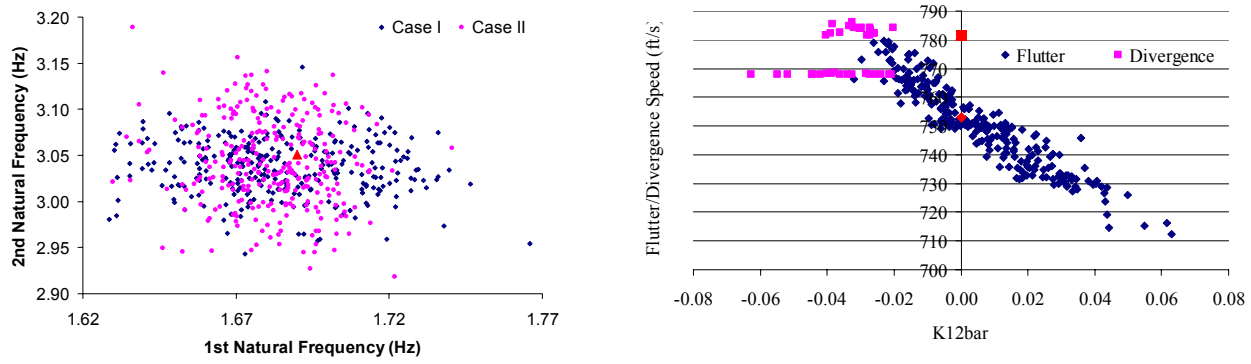

(a) (b)

Figure 6. (a) Ensemble of first and second natural frequencies, case I and II. (b) Shotgun plot of the flutter speed vs. normalized stiffness coefficient K_{12}, case I. The red triangle/square denote the design conditions (flutter/divergence).

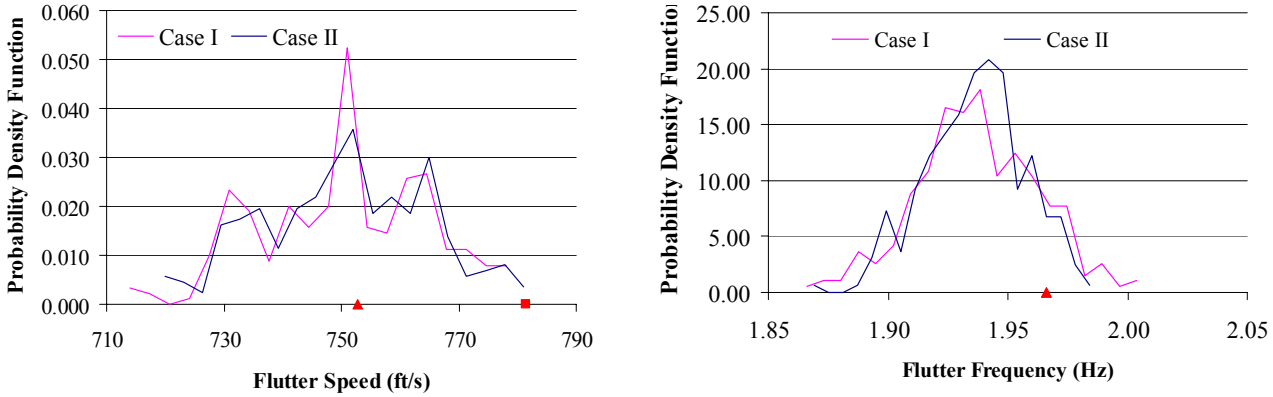

(a) (b)

Figure 7. Probability density functions of (a) the flutter speed and (b) the flutter frequency for both cases I and II. The red triangle/square denote the design conditions (flutter/divergence).

Comparing this latter case with either case I or II leads to the conclusion that the decrease of the standard deviation of one natural frequency (from 1.5% to 1%) may induce an increase, albeit small (from 0.20 to 0.22), in the standard deviation of K_{12}. To better understand this observation, note first that a uniform variation over the wing of the Young's modulus by 2% from the design value would induce a similarly uniform change of the natural frequencies by 1%. Since the mode shapes would not be altered in this process, the corresponding stiffness coefficient K_{12} would remain equal to 0. Thus, selecting equal standard deviations of the first two natural frequencies (as implicitly done in the first example) allows the occurrence of situations in which these variations are obtained through a Young's modulus increase and thus with zero or small values of K_{12} resulting. When selecting different standard deviations of the two natural frequencies, such occurrences are much more infrequent and the changes in natural frequencies are more likely to be accommodated through higher values of K_{12} as observed in Fig. 6(b).

The increase in variance of the stiffness coefficient K_{12} with respect to the previous set of computations leads not only to a higher probability of values below the negative threshold corresponding to the switch of flutter to divergence but also to a higher probability of large positive values which are associated with low flutter speeds and frequencies. These effects lead to an increase in the tails (especially the low one) of the distribution of both the flutter speed and flutter frequency, compare Figs 5 and 7, and result in a decrease of the mean values (750.59/750.80 ft/s for the speed and 1.937/1.936 Hz for the frequency, for cases I/II).

Comparing the results of Figs 7 obtained in connection with cases I and II, it appears that the statistical distribution of the flutter speed is essentially the same in both cases but that the variance of the flutter frequency is smaller in case II than in case I (by about 25%). This latter observation seems consistent with the dominance of the first mode in the flutter mode and the lower standard deviation of the first natural frequency in case II as compared to case I. The former one however stems most likely from the very strong relation between the flutter speed and K_{12} value (see Figs 6(b) and 4(a)) and the fact that the distribution of K_{12} values obtained in cases I and II are very similar (see earlier comment). Note finally that this last similarity is not surprising as K_{12} plays a symmetric role in regards to the first two natural frequencies.

Some recent efforts in the nonparametric modeling of uncertainty [8] have focused on the explicit representation of uncertainty in boundary conditions. This approach has been addressed through a Craig-Bampton substructuring strategy in which the boundary and internal degrees-of-freedom are first separated and in which the infinite stiffness imposed on the fixed boundaries is replaced by a random stiffness matrix exhibiting a large mean and constructed according to Eqs (3)-(7). If desired, the uncertainty in boundary conditions can also be combined in this methodology with uncertainty in the rest of the structural domain. These concepts were successfully applied here to the Goland wing model of Fig. 2 considering only uncertainty in the boundary conditions. As before, an ensemble of 300 uncertain wings were then simulated and their flutter/divergence boundary were determined using ZAERO for M_∞=0.7. Shown in Fig. 8(a) are the first and second natural frequencies of these wings which are all lower than their design counterparts corresponding to the perfectly clamped boundary conditions. The mean and standard deviations of these random natural frequencies were 99% and 0.27% (first natural frequency) and 99.5% and 0.13% (second natural frequency) of their design counterparts. Associated with the small variances of the natural frequencies are also small values of the stiffness coefficient K_{12} which are too small in magnitude to induce a switch to divergence. Note however that the 300 cases can be separated into two groups exhibiting either high or low flutter speed and frequency (see Fig. 8(b)). A clarification of this behavior can be achieved, as above, in terms of the random stiffness coefficients but is more complex as it involves K_{11}, K_{22}, and K_{12} at least. Finally, note the probability density functions of the flutter speed and flutter frequency, see Fig. 9. Consistently with the discussion of the previous paragraph, the flutter speeds are, as K_{12}, distributed approximately symmetrically with respect to the design value while the lowering of all natural frequencies with respect to their design values leads to a similar lowering of the flutter frequencies.

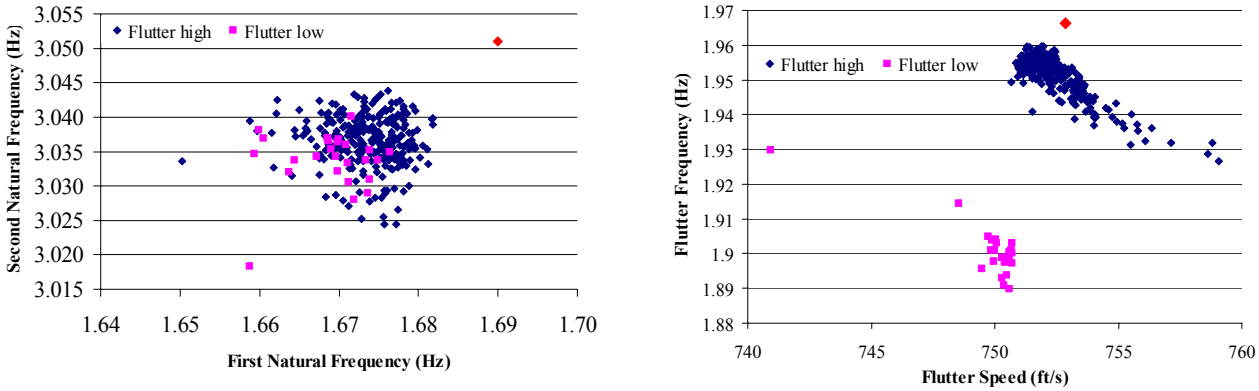

(a) (b)

Figure 8. Shotgun plot of (a) first and second natural frequencies, (b) flutter frequency vs. flutter speed, random boundary conditions. The red triangle/square denote the design conditions (flutter/divergence).

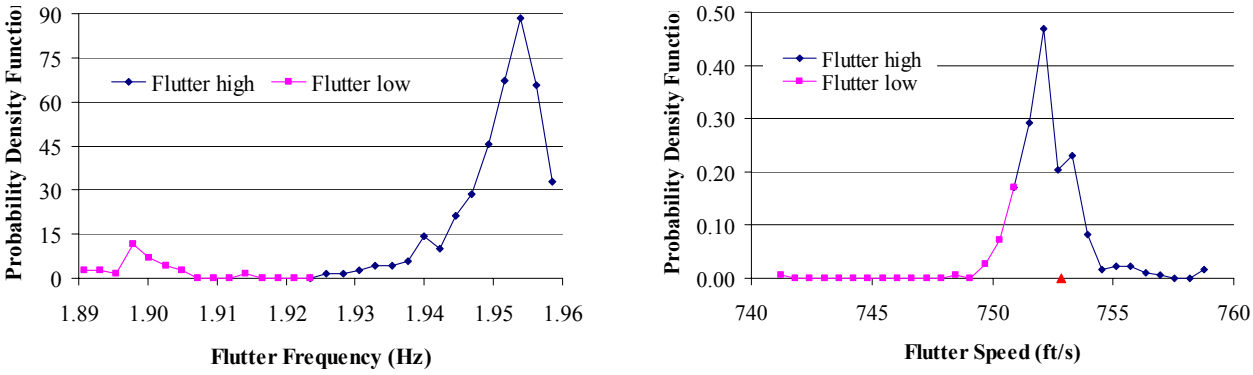

(a) (b)

Figure 9. Probability density functions of (a) the flutter frequency and (b) the flutter speed, random boundary conditions. The red triangle/square denote the design conditions (flutter/divergence).

4 AEROELASTIC APPLICATION 2: PANEL IN SUPERSONIC FLOW

The previous section has focused on the application of several variants of the nonparametric stochastic modeling of uncertainty to a specific aeroelastic problem, i.e. the flutter boundary of the Goland wing. It is next desired to demonstrate the applicability of the nonparametric methodology, the standard approach of Eqs (3)-(7) will be adopted here, to the broad class of aeroelastic problems, i.e. flutter boundary, post-flutter limit cycle oscillations, and forced response to gust/acoustic excitation. The structural system considered here is the flexible panel simply supported on an infinite wedge considered in [9], see Fig. 10. The panel width is itself infinite to maintain the

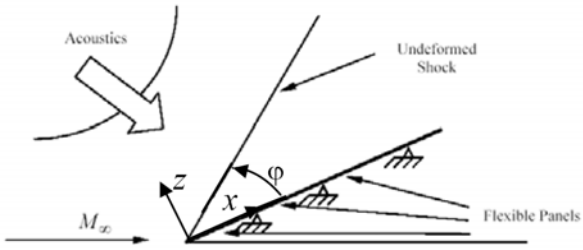

Figure 10. Aeroelastic system under consideration

two-dimensionality of both structural response and aerodynamic flow field. The wedge is placed in an upstream supersonic flow and the flow field aft shock is solved by a perturbed Euler methodology based on the characteristics of the resulting linear governing equation (see [10] for formulation and validation and [9] for a brief review). A complete aeroelastic analysis of the system is reported in [9] for a 2° semi wedge angle and M_∞=5 and it is desired here to proceed with a similar study considering uncertainty. Consistently with the analysis of [9], a three-mode modal model was selected and the parameter λ of the nonparametric stochastic modeling of the stiffness matrix, Eqs (3)-(7), was selected to achieve a standard deviation of the first natural frequency of the panel equal to 1% of its design value.

The effects of the structural uncertainty on the flutter boundary were first considered and shown in Fig. 11(a) are the flutter altitudes and flutter speeds obtained for the 1000 random panels considered. As in the Goland wing example, it is seen that a few outliers are observed that exhibit a significantly larger flutter frequency than the design condition. A correlation analysis with the random stiffness coefficients was performed again but appears more complex than in the Goland wing case. In fact, it was observed that the most significant of these coefficients in predicting the flutter frequency is K_{22}, see Fig. 11(b) but the occurrence of the outliers appears to be again associated with values of K_{12} below a specified threshold.

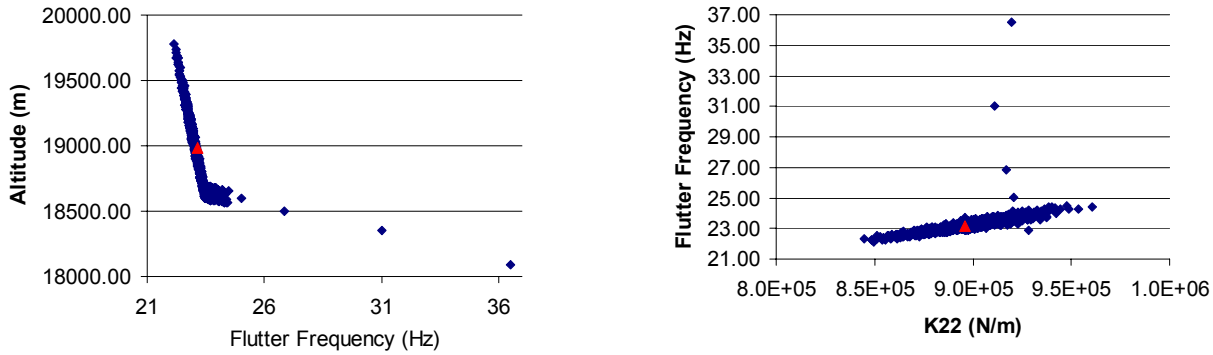

(a) (b)

Figure 11. Shotgun plots of (a) the flutter altitude vs. flutter frequency and (b) flutter frequency vs. stiffness coefficient K_{22}. The red triangle denotes the design conditions.

The forced response of the uncertain aeroelastic system to gust and/or an acoustic excitation is also of interest and it is dictated by the magnitude of the transfer function of the combined system when a linear structural model is adopted. To perform these computations, a harmonic excitation of frequency ω and unit magnitude uniformly distributed over the panel was considered and the corresponding steady state responses at the locations x= 0.3L and x= 0.5L were evaluated as a function of ω. Shown in Fig. 12 are the response vs. frequency curves corresponding to the mean model, the mean of the 1000 random responses, as well as their 2% and 98% percentiles for both locations at an altitude of 20,000m and assuming a 1% damping ratio on all modes. Note first the generally very close agreement between the mean response and the response of the mean model which differ only slightly at the resonances. Also noteworthy are the flatten peaks of the 98% percentile which arise from the varying resonances of the 1000 different panels, and the varying width of the band of uncertainty separating the 2% and 98% percentile curves.

A high fidelity nonlinear reduced order model of the panel structural deformations of the form of Eq. (1) was successfully determined in [9] and used to estimate the amplitude of the limit cycle oscillations encountered past flutter at different altitudes. It is again desired to assess the effects of structural uncertainty on these LCO

amplitudes. As described earlier, the simulation of random nonlinear geometric reduced order models is carried out through the generation of positive definite symmetric matrices $\underline{\underline{K}}_B$, see Eq. (2), so that all stiffness coefficients, linear and nonlinear, are random. This process was implemented here with λ selected again to achieve a standard deviation of the first linear natural frequency equal to 1% of its design value. A population of 500 undamped panels were selected and their LCO amplitudes were determined as a function of altitude, see Fig. 13.

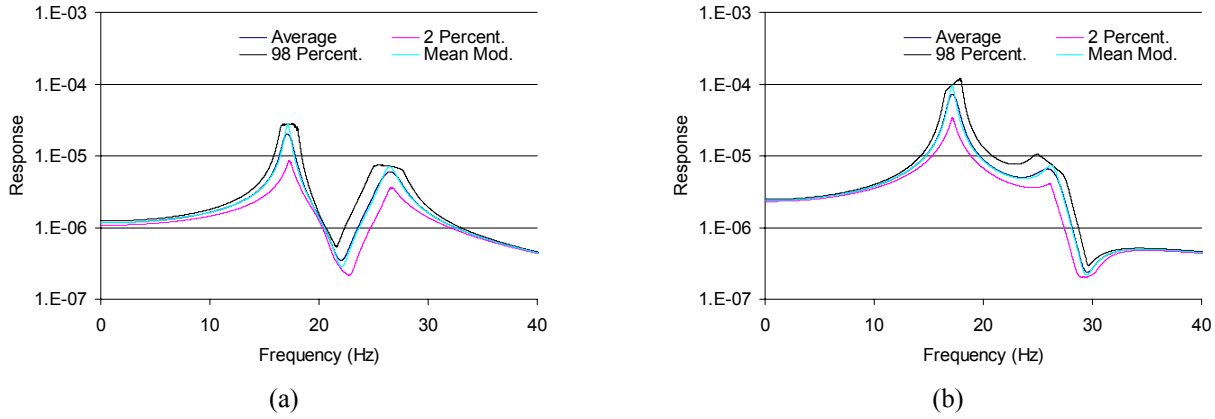

Figure 12. Steady state response vs. frequency curves corresponding to the mean model, the average of the 1000 random responses, as well as their 2% and 98% percentiles for (a) *x*= 0.3*L* and (b) *x*= 0.5*L*.

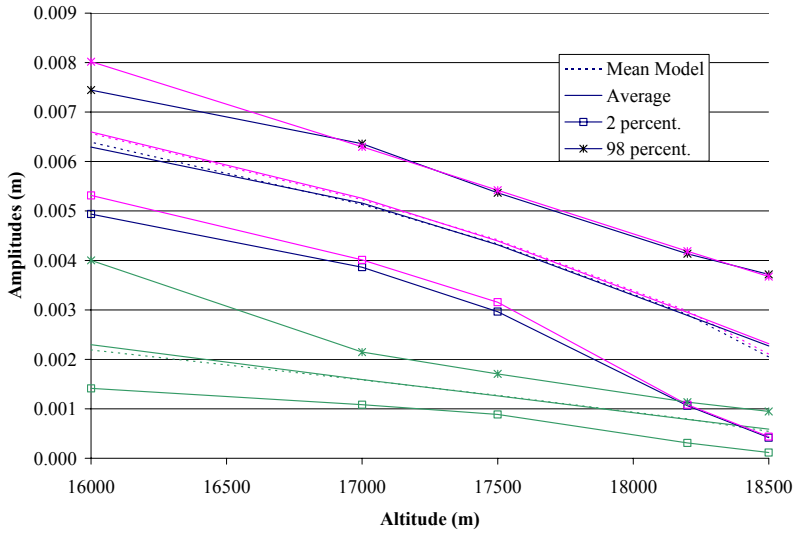

Figure 13. Amplitudes of post-flutter limit cycle oscillations vs. altitude for the three modes for the mean model, the average of the 500 random amplitudes, as well as their 2% and 98% percentiles (mode 1 in blue, mode 2 in pink and mode 3 in green).

In this regard, note first that not all 500 panels did flutter at 18200m and 18500m, as can be expected from Fig. 11(a). In fact, there were 77 at 18500m and 9 at 18200m that did not and thus these 86 data points were not used in producing Fig. 13. A strong correlation between amplitude of LCO and value of the stiffness coefficient K_{22} was again generally observed consistently with the results of Fig. 11(b), see Fig. 14.

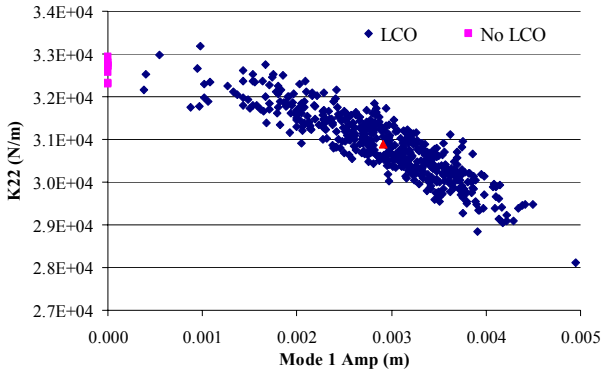

Figure 14. Shotgun plot of the LCO amplitude of mode 1 vs. stiffness coefficient K_{22}, 18200m. The red triangle denotes the design conditions.

As already seen in Fig. 12, note that the LCO amplitude of the mean model and the average of the LCO amplitudes obtained for all samples are close to each other over the entire range of altitudes considered. Further, except for mode 3 at 16000m, it appears that the band of uncertainty between the 2% and 98% percentiles remains approximately constant over the range of altitudes. The sudden increase of the 98% percentile of mode 3 at 16000m is associated with the occurrence of a new type of LCO in some of the 500 cases considered. Specifically, these new solutions exhibit an asymmetry and significant multi harmonic contributions as seen in Fig. 15(a) at the contrary of the symmetric, strongly single harmonic motions occurring in particular for the design condition, see Fig. 15(b). Further, the asymmetry appears to induce a significant increase in peak response of mode 2 and, especially, mode 3.

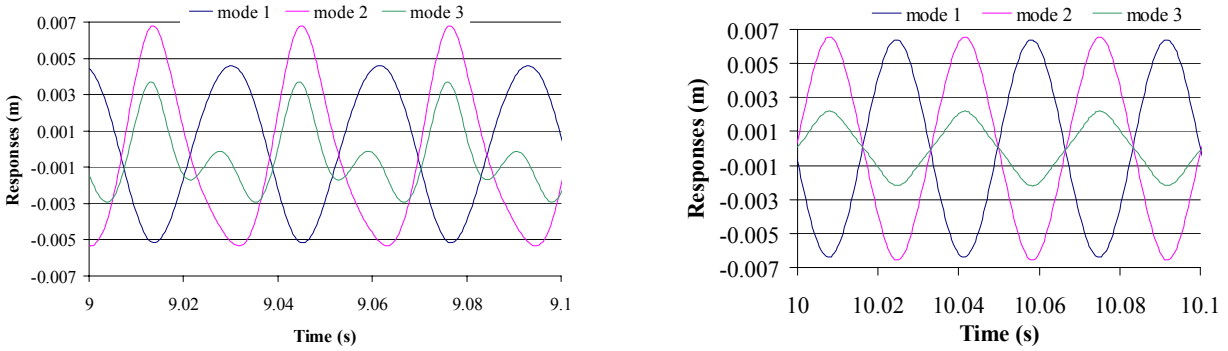

Figure 15. Some limit cycle oscillations occurring at 16000m. (a) Asymmetric solution of a random panel. (b) Symmetric solution of the design condition.

The last aeroelastic problem to be considered here is the post-flutter response of the panel to an external acoustic excitation. To this end, each of the 500 panels was subjected to a white noise excitation of sound pressure level of 121.8dB (or 144.8dB OASPL) and the corresponding spectra of the nonlinear response were determined at both $x= 0.3L$ and $x= 0.5L$. Shown in Fig. 16 are the spectra corresponding to the mean model, the mean of the 500 random spectra, as well as their 2% and 98% percentiles for both locations at an altitude of 17,000m. As observed already in connection with the linear response and the LCO results, note the very

close agreement between the mean response and the response of the mean model over the entire frequency range of interest. Note finally the broad changes of the uncertainty band between the 2% and 98% percentile curves from which it is concluded that the uncertainty affects differently different resonances.

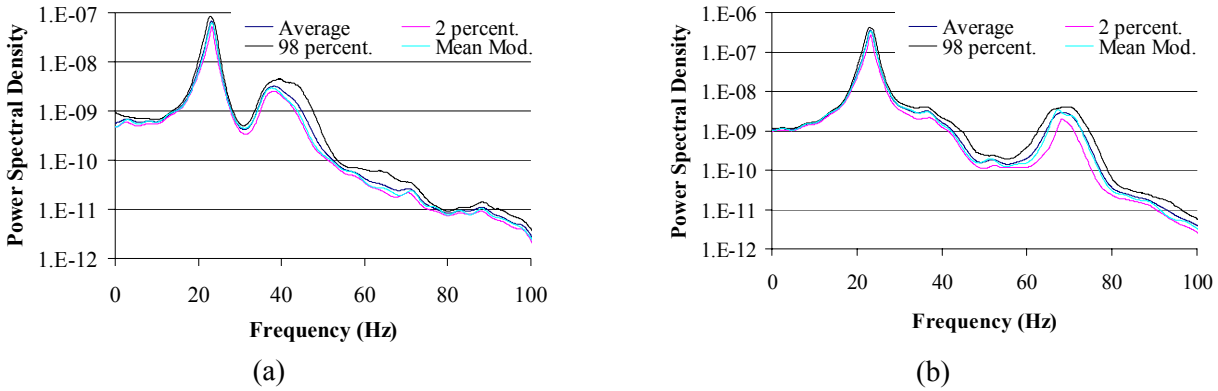

Figure 16. Power spectral densities of the nonlinear response of the mean model, the average of the 500 random spectra, as well as their 2% and 98% percentiles for (a) *x*= 0.3*L* and (b) *x*= 0.5*L*.

5 SUMMARY

The focus of this investigation has been on the introduction and the successful validation of a general framework for the consideration of structural uncertainty in aeroelastic analyses. The consideration of uncertainty was achieved directly at the level of the modal/reduced order model through the randomization of the mass, damping, and stiffness (linear and nonlinear) matrices while maintaining fixed the modal basis. The nonparametric approach, based on the maximization of the statistical entropy, was proposed for the stochastic modeling of these random matrices and a convenient algorithm for their simulation was described, see Eqs (3)-(7).

The validation of this nonparametric strategy was accomplished on two specific aeroelastic problems, the first of which is the determination of the random flutter boundary of uncertain Goland wings. Three different, complementary variants of the nonparametric approach were considered for this problem. First, the "standard" approach was utilized and the single free parameter of the model (λ) was selected so that the standard deviation of the first natural frequency of the random wings equals 1% of its counterpart for the design Goland wing. An extension of this method was considered next that allows for the imposition of variability on several quantities, e.g. on the first two natural frequencies. A final analysis was carried out with a recently proposed nonparametric method for the consideration of uncertainty in the boundary conditions. A very detailed assessment of the effects of structural uncertainty on the Goland wing flutter boundary resulted from these three sets of analyses. In particular, it was demonstrated that the random stiffness coefficient K_{12} coupling the first two modes of the design wing in the analysis of a random wing played a particular important role and could dramatically affect, even at low levels of uncertainty, the flutter boundary (speed, frequency, and mode).

The second application involved the aeroelastic response of uncertain linear and geometrically nonlinear panels in a supersonic flow. The standard nonparametric approach was selected to assess the effects of uncertainty on all aspects of the aeroelastic response, i.e. the flutter boundary, the post-flutter limit cycle oscillations, and the forced response to a gust/acoustic excitation in both linear (pre-flutter) and nonlinear

(post-flutter) response regimes. The simulation of the linear and nonlinear stiffness coefficients was accomplished with the same ease as in the Goland wing example and the results demonstrated again that the aeroelastic response can be very sensitive to even a small level of uncertainty.

6 REFERENCES

[1] Soize, C., 2000, "A Nonparametric Model of Random Uncertainties on Reduced Matrix Model in Structural Dynamics," *Probabilistic Engineering Mechanics*, Vol. 15, No. 3, pp. 277-294.

[2] Soize, C., 2001, "Maximum Entropy Approach for Modeling Random Uncertainties in Transient Elastodynamics," *Journal of the Acoustical Society of America*, Vol. 109, No. 5, pp. 1979-1996.

[3] Mignolet, M.P., and Soize, C., 2007, "Stochastic Reduced Order Models for Uncertain Nonlinear Dynamical Systems," *Proceedings of the International Modal Analysis Conference, IMAC XXV*, Orlando, Florida, Feb. 19-22.

[4] Mignolet, M.P., and Soize, C., 2006, "Nonparametric Stochastic Modeling of Linear Systems with Prescribed Variance Information of Several Natural Frequencies," *Proceeding of the Fifth International Conference on Computational Stochastic Mechanics*, Rhodes, Greece, Jun. 21-23. To appear in *Probabilistic Engineering Mechanics*.

[5] Soize, C., 2005, "Random Matrix Theory for Modeling Uncertainties in Computational Mechanics," *Computer Methods in Applied Mechanics and Engineering*, Vol. 194, pp. 1333-1366.

[6] Goland, M., and Luke, Y., 1948, "The Flutter of a Uniform Wing with Tip Weights," *Journal of Applied Mechanics*, Vol. 15, No. 3, pp. 13-20.

[7] Eastep, F.E., Khot, N.S., Beran, P.S., Zweber, J.V., and Snyder, R.D., 2002, "Investigation of Shock-Induced LCO of a Wing/Store Configuration Using the Transonic Small Disturbance Method," Proceedings of the 23rd Congress of the International Council on the Aeronautical Sciences (ICAS), Toronto, Canada, Sept. 8-13.

[8] Mignolet, M.P., and Soize, C., 2007, "Nonparametric Stochastic Modeling of Structural Dynamic Systems with Uncertain Boundary Conditions," *Presented at the 9th U.S. National Congress on Computational Mechanics*, San Francisco, California, Jul. 23-26.

[9] Kim, K., Kim, Y.C., Mignolet, M.P., Liu, D.D., Chen, P.C., Lee, D.H., 2007, "Random Aeroelastic Response Due to Strong Hypersonic Unsteady-Wave/Shock Interaction with Acoustic Loads," *Proceedings of the 48th Structures, Structural Dynamics, and Materials Conference*, Honolulu, Hawaii, Apr. 23-26. AIAA Paper AIAA-2007-2014.

[10] Chavez, F.R. and Liu, D.D., 1995, "Unsteady Unified Hypersonic/Supersonic Method for Aeroelastic Applications Including Wave/Shock Interaction," *AIAA Journal*, Vol. 33, No. 6, pp. 1090-1097.

Paper No. 2

Discusser's Name: D. Pitt

Question: I think for the Goland wing, if we were to manufacture 300 wings as you simulated, that all 300 wings would, when tested, result in diagonalized generalized mass and generalized stiffness matrices. Yet, your simulations showed coupled matrices.

Author's Reply: The nature, diagonal or coupled, of the generalized mass and stiffness matrices of the manufactured wings depends on the modes selected to represent their motions. If one adopts for each wings its own modes, then you are correct – the generalized mass and stiffness matrices will be diagonal. Here, however, we have adopted the modes of the mean (or baseline) wing because this choice leads to a much more tractable uncertainty analysis, as described in the introduction of the paper. When adopting these modes, the generalized mass and stiffness matrices will be coupled. Note that one can pass back and forth from the diagonal matrices (when using the modes of each wing) to the coupled matrices (when using the modes of the mean/baseline wing) by expressing the modes of each wing in terms of the modes of the mean/baseline wing.